PHYSICAL REVIEW D VOLUME 23, NUMBER 1 1 JANUARY 1981

W and Z^0 decays into quarks plus a photon or a gluon

T. R. Grose* and K. O. Mikaelian†
Department of Physics, Oklahoma State University, Stillwater, Oklahoma 74078
(Received 28 August 1980)

We study the decays $W\to q\bar{q}\gamma$, $W\to q\bar{q}g$, $Z^0\to q\bar{q}\gamma$, and $Z^0\to q\bar{q}g$ within a unified approach. Several interesting properties such as asymmetries in the decay spectra, vanishing Dalitz plots, etc., are found in $W\to q\bar{q}\gamma$ and traced to the presence of a W-γ-W coupling as given by gauge theories. We derive and compare differential and total decay rates for processes with and without such a triple-boson coupling which in general acts as a suppression factor. Three-jet decays $W\to q\bar{q}g$ and $Z^0\to q\bar{q}g$, not suppressed by such a coupling, have appreciable branching ratios. The possibility of studying more exotic three-jet decays such as $Z^0\to ggg$ is discussed briefly.

I. INTRODUCTION

It is expected that in the next decade several high-energy machines which are now under construction or serious study will begin operating at energies sufficient to produce the weak intermediate vector bosons $W^\pm$ and Z^0. Their discovery will fulfill early predictions,[1] while the measurement of their masses and production cross sections will serve as further tests of the standard Weinberg-Salam model.[2] More critical tests of the model, in particular the search for the triboson couplings, can be studied[3] in pair production or associated production like W^+W^-, $W^\pm Z^0$, and $W^\pm\gamma$.

Assuming that a rich source of intermediate vector bosons is found in the not too distant future, we may turn towards the study of specific decay processes which will yield more information than the basic W-q-$\bar{q}$ and Z^0-q-$\bar{q}$ couplings. In this paper, we present the differential and the total decay rates for

(i) $W\to q+\bar{q}+\gamma$,

(ii) $W\to q+\bar{q}+g$,

(iii) $Z^0\to q+\bar{q}+\gamma$,

and

(iv) $Z^0\to q+\bar{q}+g$.

We refer to these processes as "three-jet decays of the W and the Z^0" and borrow the terminology commonly used in describing three-jet events[4] in e^+e^-; instead of the decay of a massive virtual photon, we are studying the decay of a massive real W or Z^0 into quarks, antiquarks, and gluons or photons.

Our calculations are based on the standard Weinberg-Salam model and quantum chromodynamics. Within this framework we find the interesting result that in the limit of massless quarks all four amplitudes can be expressed as a universal factor (later to be called the Abelian amplitude) times a second factor which depends on the reaction and which contains the coupling constants, etc. Of course, it is no surprise that reactions (ii), (iii), and (iv) are all simply related because they all proceed by similar Feynman diagrams (Fig. 1), but it is surprising that $W\to q\bar{q}\gamma$, Fig. 2, can also be expressed in a similar fashion. In this case, we find that the second factor is nontrivial and, in fact, it contains a zero along a certain line in the Dalitz plot. The existence of such a zero seems to require a triboson coupling since nothing similar happens in (ii), (iii), or (iv) where the triboson coupling is absent.

In the next section we write down the amplitude for (i) and discuss its factorization properties. The doubly differential decay rate is then calculated and Dalitz plots presented for the example of $W^-\to d\bar{u}\gamma$. After two integrations the total decay rate is obtained. In Sec. III we consider $W\to q\bar{q}g$, and in Sec. IV we treat $Z^0\to q\bar{q}\gamma$ and $Z^0\to q\bar{q}g$. Conclusions and comparisons among the four different processes are given in Sec. V. In Appendix A we briefly show that in the case of spin-0 quarks the Abelian amplitude is different but the second factor, and hence the position of the zero, is the same as in the case of the standard spin-$\frac{1}{2}$ quarks. In Appendix B we give the results for a more general W-γ-W coupling.

II. $W\to Q_i\bar{Q}_j\gamma$

In Fig. 2 we show the Feynman diagrams and the particle momenta for the decay $W\to q_i\bar{q}_j\gamma$. We have in mind, for example, $W^-\to d\bar{u}\gamma$, though we make

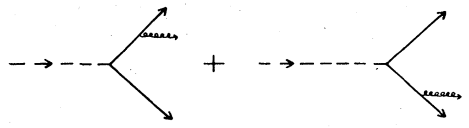

FIG. 1. Feynman diagrams for $Z^0\to q\bar{q}g$ and $W\to q\bar{q}g$. Similar diagrams contribute to $Z^0\to q\bar{q}\gamma$.

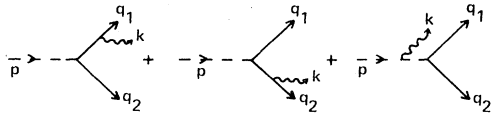

FIG. 2. Feynman diagrams for $W\to q\bar{q}\gamma$ showing the particle momenta.

the following generalization: let the charge of the W, q_i, and $\bar{q}_j$ be Q, Q_i, and Q_j, respectively, with $Q=Q_i+Q_j$ from (electric) charge conservation, e.g., $-1=-\frac{1}{3}-\frac{2}{3}$. Since we drop all quark masses, this will allow us to apply our results immediately to $W^-\to e\bar{\nu}_e\gamma$, plus we shall find that the amplitude has an interesting dependence on Q and Q_i. Other generalizations are also possible and will be pointed out as we go along.

Figure 2 gives the following amplitude:

$$\mathfrak{M}=\frac{-ieg}{2\sqrt{2}}\epsilon_\gamma^\mu\epsilon_W^\nu\bar{u}(q_1)\Big\{Q_i\gamma_\mu\frac{1}{\not l_1-m_1}\gamma_\nu(1-\gamma_5)+Q_j(1+\gamma_5)\gamma_\nu\frac{1}{\not l_2+m_2}\gamma_\mu$$
$$+\frac{Q(1+\gamma_5)}{h^2-M_w^{\,2}}\gamma_\alpha\left(g^{\alpha\beta}-\frac{h^\alpha h^\beta}{M_w^{\,2}}\right)[2p_\mu g_{\nu\beta}+(h-2p)_\beta g_{\mu\nu}+(p-2h)_\nu g_{\beta\mu}]\Big\}v(q_2)\,. \tag{1}$$

One can easily check that this amplitude is gauge invariant ($\mathfrak{M}\to 0$ if $\epsilon_\gamma^\mu\to k^\mu$) provided that $Q=Q_i+Q_j$. We have used the following definitions: $l_1=p-q_2=k+q_1$, $l_2=p-q_1=k+q_2$, and $h=p-k=q_1+q_2$.

Dropping the quark masses m_1 and m_2, and using $k_\mu\epsilon_\gamma^\mu=p_\mu\epsilon_W^\mu=\bar{u}(q_1)\not q_1=\not q_2 v(q_2)=0$, Eq. (1) reduces to

$$\mathfrak{M}=\frac{-ieg}{2\sqrt{2}}\epsilon_\gamma^\mu\epsilon_W^\nu\bar{u}(q_1)\left[Q_1\gamma_\mu\frac{1}{\not l_1}\gamma_\nu+Q_j\gamma_\nu\frac{1}{\not l_2}\gamma_\mu-\frac{Q}{k\cdot p}(p_\mu\gamma_\nu-\not p g_{\mu\nu}+k_\nu\gamma_\mu)\right](1-\gamma_5)v(q_2)\,. \tag{2}$$

The remaining algebraic steps are tedious but straightforward. The result is[5]

$$\mathfrak{M}=\frac{-ieg}{2\sqrt{2}}\left(Q_i-Q\frac{k\cdot q_1}{k\cdot p}\right)\epsilon_\gamma^\mu\epsilon_W^\nu\bar{u}(q_1)\left(\gamma_\mu\frac{1}{\not l_1}\gamma_\nu-\gamma_\nu\frac{1}{\not l_2}\gamma_\mu\right)(1-\gamma_5)v(q_2)\,. \tag{3}$$

The factorization referred to in the Introduction is clearly exhibited in Eq. (3). The Abelian factor is

$$\gamma_\mu\frac{1}{\not l_1}\gamma_\nu-\gamma_\nu\frac{1}{\not l_2}\gamma_\mu\,,$$

the same factor which occurs, for example, in $Z^0\to q\bar{q}\gamma$, and represents the sum of the two amplitudes for the emission of a photon from a quark and an antiquark of equal charge, as in Fig. 1. We repeat that Eq. (3) is valid, however, for arbitrary charges Q, Q_i, and Q_j satisfying charge conservation (we eliminated Q_j using $Q_j=Q-Q_i$). All the remaining reactions (ii), (iii), and (iv) will contain only this Abelian factor. It is interesting that the addition of the triboson (in this case $W-\gamma-W$) coupling modifies the Abelian amplitude by a nontrivial multiplicative factor $[Q_i-Q(k\cdot q_1)/k\cdot p]$. Furthermore, as we shall see, this factor vanishes in the physical region when $k\cdot q_1/k\cdot p=Q_i/Q$.

This factorization property is destroyed if one uses a triboson coupling different from the standard gauge-theory coupling. In an earlier work[6] this coupling was generalized in the traditional way of introducing[7] a magnetic moment parameter κ. The differential cross section for $\gamma q\to W^\pm q'$, calculated for arbitrary κ, was found[6] to factorize for the case $\kappa=1$, its gauge-theory value. More recently the production cross section for $q_i\bar{q}_j\to W^\pm\gamma$ was calculated with arbitrary κ and reported[8] to have a zero in the differential cross section. We can now trace these results to the factorization of the amplitude as discussed above, and point out that the condition for the zero $k\cdot q_1/k\cdot p=Q_i/Q$ sets no requirements on the spins of the particles. In fact, we show in Appendix A that the same factor is obtained for spin-0 quarks also.

The details of the remaining steps need not be given: we square the amplitude $\mathfrak{M}$, average over initial and sum over final helicities, and sum over the quark colors [for simplicity we dropped the color indices in Eqs. (1)–(3)]. Denoting the result by $\langle|\mathfrak{M}|^2\rangle$, we have for the doubly differential decay rate

$$\frac{d^2\Gamma}{dE_1dE_2}=\frac{\pi^2}{2M_W(2\pi)^5}\langle|\mathfrak{M}|^2\rangle\,, \tag{4}$$

where E_1 and E_2 are the energies of the quark and antiquark, respectively, in the W rest frame. Switching to two dimensionless variables

$$x=1-2E_2/M_W \tag{5}$$

and

$$y=1-2E_1/M_W\,,$$

we find

$$\frac{d^2\Gamma}{dx\,dy}=\frac{\alpha g^2M_W}{32\pi^2}\left(Q_i-Q\frac{x}{x+y}\right)^2\frac{(x-1)^2+(y-1)^2}{xy}\,, \tag{6}$$

where $\alpha = e^2/4\pi$ and g is the weak charge which satisfies

$$g = 2M_W(\sqrt{2}G_F)^{1/2} = e/\sin\theta_W \tag{7}$$

in the Weinberg-Salam model.[9] The corresponding decay into two quarks only has a width

$$\Gamma_0 = \Gamma(W \to q_i\bar{q}_j) = \frac{g^2 M_W}{16\pi} = \frac{G_F M_W^3}{2\sqrt{2}\pi}, \tag{8}$$

which we use for normalization and write

$$\frac{1}{\Gamma_0}\frac{d^2\Gamma}{dx\,dy} = \frac{\alpha}{2\pi}\left(Q_i - Q\frac{x}{x+y}\right)^2 \frac{(x-1)^2+(y-1)^2}{xy}. \tag{9}$$

As a check of our calculation we have compared Eq. (9) with the cross section for $q_i\bar{q}_j \to W^-\gamma$ in the case $\kappa = 1$. The result for arbitrary κ is given in Appendix B.

While x and y range between 0 and 1, we will require that each particle carry a minimum energy $E_{\min} = \epsilon M_W$, with ϵ a small number $0 < \epsilon < \frac{1}{3}$. The phase space then becomes[10]

$$\epsilon \le x \le 1 - 2\epsilon, \qquad \epsilon \le y \le 1 - x - \epsilon. \tag{10}$$

From Eq. (9) we see that within the physical region the decay rate vanishes along a line given by

$$y = \left(\frac{Q}{Q_i} - 1\right)x = \left(\frac{Q_j}{Q_i}\right)x \tag{11}$$

which reduces to $y = 2x$ for $W^- \to d\bar{u}\gamma$. Note that for $W^- \to e^-\bar{\nu}_e\gamma$, the zero occurs at the edge of the phase space, $y = 0$. From Eq. (11) it is clear that the zero will be in the physical region if and only if the condition $Q/Q_i > 1$ is satisfied, or, equivalently, if Q_i and Q_j have the same sign.

In Fig. 3 we show the Dalitz plot for $W^- \to d\bar{u}\gamma$. This has been done by breaking the phase space in the x-y plane into small squares of size 0.05×0.05 and integrating Eq. (9) numerically over each square. The number of points assigned is proportional to the contribution of this integral over each square. In the same figure we also show the line, Eq. (11), along which the decay rate vanishes. We find that around that line the decay rate remains so small as to contribute less than a point per square area, which we leave blank. The sum of all such fractional points from that region comes up to about 4 out of a total of 200 points used in Fig. 3.

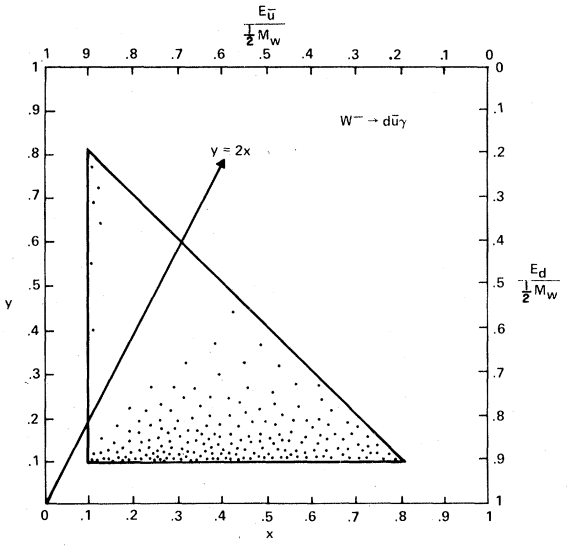

FIG. 3. Dalitz plot for $W^- \to d\bar{u}\gamma$ with the cutoff $\epsilon = 0.1$. The axes are labeled by x and y or, equivalently, by $E_{\bar{u}}$ and E_d normalized to their maximum value $\frac{1}{2}M_W$. Also shown the line $y = 2x$ along which the doubly differential decay rate vanishes identically.

More quantiatively, we plot $(1/\Gamma_0)d^2\Gamma/dx\,dy$ as a function of x for two values of y in Fig. 4, and as a function of y for two values of x in Fig. 5. Note that the asymmetry between x and y, which can be seen by comparing Fig. 4 with Fig. 5, is due to the fact that the charge of the W is split in an asymmetric way; in other words, the energies of the quark and antiquark are different because their charges are different. Only for $Q_i = Q_j = Q/2$ would the two distributions be identical [see Eq. (9)].

After one integration we obtain the singly differential decay distributions $d\Gamma/dx$ or $d\Gamma/dy$. We find

$$\frac{1}{\Gamma_0}\frac{d\Gamma}{dy} = \frac{\alpha}{2\pi}\left\{Q_i^2\left[(y-2+2/y)\ln\left(\frac{1-y-\epsilon}{\epsilon}\right) - (1+3/y)(1-y-2\epsilon)/2\right]\right.$$
$$- QQ_i\left[4(y+1/y)\ln\left(\frac{1-\epsilon}{y+\epsilon}\right) - 3(1+1/y)(1-y-2\epsilon)\right] + 2Q^2(1+2y+1/y)\ln\left(\frac{1-\epsilon}{y+\epsilon}\right)$$
$$\left. - \frac{Q^2(1-y-2\epsilon)}{2(y+\epsilon)}\left[5y + 3\epsilon/y + \frac{4y^2}{1-\epsilon} + (7-5\epsilon)(1+\epsilon)/(1-\epsilon)\right]\right\}. \tag{12}$$

One can show that to obtain $1/\Gamma_0\, d\Gamma/dx$ all that is needed is to let $y \to x$ and $Q_i \to Q_j$ in the above expression:

$$\frac{1}{\Gamma_0}\frac{d\Gamma}{dx}=\left(\frac{1}{\Gamma_0}\frac{d\Gamma}{dy}\right)_{y\to x,\,Q_i\to Q_j}. \tag{13}$$

These two distribution functions are shown in Fig. 6. The asymmetry between the x and y distributions is quite striking, meaning there is a large difference between the energies of the d and $\bar{u}$ in $W^-\to d\bar{u}\gamma$, with d, on the average, carrying more energy than the $\bar{u}$. As we will see in the next section, there is no such asymmetry for $W\to d\bar{u}g$, also shown in Fig. 6.

Finally, a second integration gives the total decay rate Γ as a function of Q, Q_i, and ϵ:

$$\Gamma/\Gamma_0=\frac{\alpha}{2\pi}\left\{(Q_i^2+Q_j^2)\left[\ln^2\left(\frac{\epsilon}{1-\epsilon}\right)+\tfrac{3}{2}(1-2\epsilon)\ln\left(\frac{\epsilon}{1-2\epsilon}\right)-\pi^2/6+\tfrac{1}{4}(5+3\epsilon)(1-3\epsilon)+2\,\mathrm{Li}_2\left(\frac{\epsilon}{1-\epsilon}\right)\right]\right.$$
$$\left.+\frac{Q^2}{1-\epsilon}(1-3\epsilon)(\tfrac{11}{3}-\epsilon^2)+2Q^2(1+\epsilon)^2\ln\left(\frac{2\epsilon}{1-\epsilon}\right)\right\}. \tag{14}$$

As a check, we note that the above expression vanishes as it should if we set $\epsilon=\frac{1}{3}$. The branching ratios Γ/Γ_0 for $W^-\to d\bar{u}\gamma$ and $W^-\to e\bar{\nu}_e\gamma$ are shown in Fig. 7 as a function of the cutoff parameter ϵ.

Our discussion of the radiative decays of W bosons is now complete. As we shall see in the next two sections, the remaining decays (ii)–(iv) can be obtained in a rather straightforward manner from the results derived in this section.

III. $W\to Q_i\bar{Q}_jG$

In the absence of a W-g-W coupling only two diagrams, shown in Fig. 1, contribute to the decay $W\to q_i\bar{q}_jg$. The decay amplitude is

$$\mathfrak{M}=\frac{-ig_sg}{2\sqrt{2}}\,\epsilon^{\mu}_{\text{gluon}}\epsilon^{\nu}_{W}T^a_{ji}\bar{u}_i(q_1)\left(\gamma_\mu\frac{1}{\not{l}_1}\gamma_\nu-\gamma_\nu\frac{1}{\not{l}_2}\gamma_\mu\right)(1-\gamma_5)v_j(q_2), \tag{15}$$

where we have included all color indices. Comparing with Eq. (3), we see that apart from the color matrix T^a the replacement $Q\to 0$ and $eQ_i\to g_s$ will take us from the photon case to the gluon case.

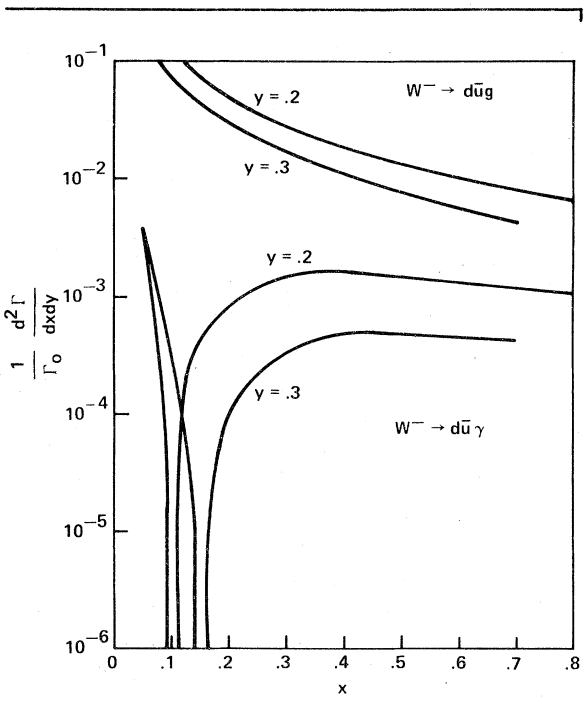

FIG. 4. The doubly differential decay rate $d^2\Gamma/dx\,dy$ for $W^-\to d\bar{u}g$ and $W^-\to d\bar{u}\gamma$ as a function of x for $y=0.2$ and $y=0.3$, normalized to $\Gamma_0=\Gamma(W^-\to d\bar{u})$. To describe $Z^0\to q\bar{q}g$, $e^+e^-\gamma$, $u\bar{u}\gamma$, and $d\bar{d}\gamma$ the upper curves must be multiplied by 1, $\frac{3}{4}$, $\frac{1}{3}$, and $\frac{1}{12}$, respectively (see text). For gluons the curves must be multiplied by the additional factor $\alpha_s/\alpha\approx 25$.

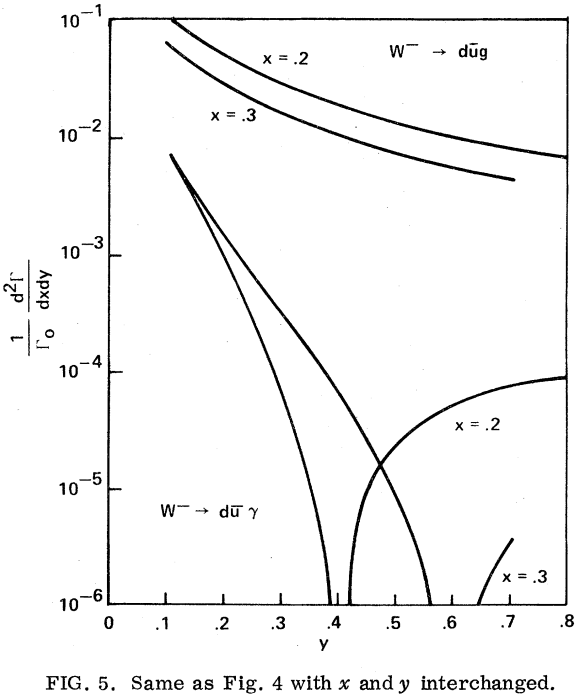

FIG. 5. Same as Fig. 4 with x and y interchanged.

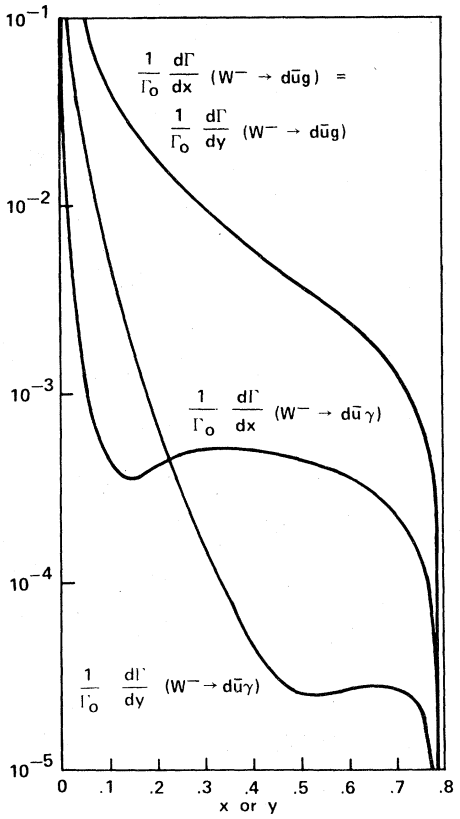

FIG. 6. The differential decay rates $d\Gamma/dx$ and $d\Gamma/dy$ for $W^- \to d\bar{u}g$ and $W^- \to d\bar{u}\gamma$, normalized to $\Gamma_0 = \Gamma(W^- \to d\bar{u})$. For $Z^0 \to q\bar{q}g$, $e^+e^-\gamma$, $u\bar{u}\gamma$, and $d\bar{d}\gamma$ multiply the upper curve by 1, $\frac{3}{4}$, $\frac{1}{3}$, and $\frac{1}{12}$, respectively. The gluon curves must be multiplied by $\alpha_s/\alpha \approx 25$. The cutoff $\epsilon = 0.1$.

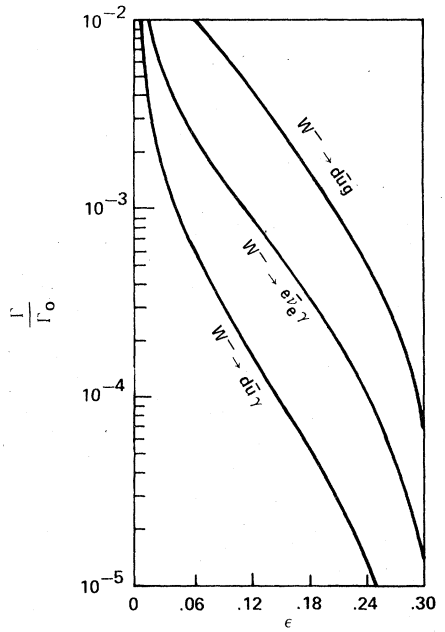

FIG. 7. The branching ratios for $W^- \to d\bar{u}g$, $W^- \to e\bar{\nu}_e\gamma$, and $W^- \to d\bar{u}\gamma$ as a function of the cutoff ϵ. The upper curve, which must be multiplied by $\alpha_s/\alpha \approx 25$ for decays with gluons, also describes Z^0 decays—see caption under Fig. 6.

The presence of T^a means that the color sum over the final states gives a factor 4 instead of 3. Therefore [see Eq. (9)].

$$\frac{1}{\Gamma_0}\frac{d^2\Gamma}{dx\,dy} = \frac{2\alpha_s}{3\pi}\frac{(x-1)^2+(y-1)^2}{xy}, \tag{16}$$

where α_s is the strong running coupling constant. This expression agrees with the result of Rizzo[11] and, except for an overall constant, is identical to the jet-energy distribution[4,12] in $e^+e^- \to 3$ jets based on $e^+e^- \to q\bar{q}g$. It is reasonable, and consistent with recent experimental data,[13] to take

$$\alpha_s = \alpha_s(M_W^2) = \frac{12\pi}{(33-2f)\ln(M_W^2/\Lambda^2)} \tag{17}$$

which is about 0.18 for $f=6$, $M_W = 80$ GeV/c^2, and $\Lambda = 0.5$ GeV/c^2. We will later use this value for numerical results, but we point out that all we need to calculate the branching ratio is the assumption, as of course made in $e^+e^- \to 3$ jets, that α_s is a function of only the c.m. energy and is independent of x and y. Then we find

$$\frac{\Gamma}{\Gamma_0} = \frac{4\alpha_s}{3\pi}\left[\ln^2\left(\frac{\epsilon}{1-\epsilon}\right) + \tfrac{3}{2}(1-2\epsilon)\ln\left(\frac{\epsilon}{1-2\epsilon}\right) - \frac{\pi^2}{6} + \tfrac{1}{4}(5+3\epsilon)(1-3\epsilon) + 2\,\mathrm{Li}_2\left(\frac{\epsilon}{1-\epsilon}\right)\right]. \tag{18}$$

To compare with earlier work, we expand the above expression for small ϵ:

$$\frac{\Gamma}{\Gamma_0} = \frac{4\alpha_s}{3\pi}\left[\ln^2\epsilon - \tfrac{3}{2}\left|\ln\epsilon\right| + \tfrac{5}{4} - \pi^2/6 + \epsilon\left|\ln\epsilon\right| + 2\epsilon + O(\epsilon^2)\ldots\right], \tag{19}$$

which agrees with the result obtained[4,12] in $e^+e^- \to q\bar{q}g$.

We will not go into the detailed rewriting of the doubly differential decay rate in terms of thrust, spherocity, etc. (see, e.g., Ref. 11). Obviously, one can apply the full machinery of three-jet events to $W \to q\bar{q}g$ and $Z^0 \to q\bar{q}g$. Our interest is to compare the Abelian and the non-Abelian amplitudes; for this purpose we have included in Figs. 4—7 several curves describing $W \to d\bar{u}g$.

Two observations concerning these curves need to be made: First, the symmetry between quarks and antiquarks is apparent for decays with gluons —see Eq. (16). Second, even *after* taking out the

factor $\alpha_s/\alpha \sim 25$ as has been done in Figs. 4—7, the results for the gluon case remain larger than the photon case, apparently because the factor $[Q_i - Qx/(x+y)]^2$ suppresses the photon mode, a suppression which persists even after integrating over x and y.

IV. $Z^0 \to Q_i\bar{Q}_i\gamma$ AND $Z^0 \to Q_i\bar{Q}_iG$

These decays differ from W decays in only two aspects: the charge of the Z^0 is zero (hence, we set $Q=0$), and the basic coupling of the Z^0 to the $q_i\bar{q}_i$ is different. We wrote[9] $g/2\sqrt{2}\,\gamma_\mu(1-\gamma_5)$ for the q_i-W-q_j vertex, where g is given by Eq. (7). For q_i-Z^0-q_i, we use the vertex

$$2^{1/4}M_Z\sqrt{G_F}\,\gamma_\mu(a^i - b^i\gamma_5).$$

In the standard model $a^u = a^c = a^t = \frac{1}{2} - \frac{4}{3}\sin^2\theta_W$, $a^d = a^s = a^b = -\frac{1}{2} + \frac{2}{3}\sin^2\theta_W$, $a^e = a^\mu = a^\tau = -\frac{1}{2} + 2\sin^2\theta_W$, and $b^u = b^c = b^t = -b^d = -b^s = -b^e = -b^\mu = -b^\tau = \frac{1}{2}$. For neutrinos, $a^\nu = b^\nu = \frac{1}{2}$. The decay width into two fermions is given by

$$\Gamma_0 = \Gamma(Z^0 \to l_i\bar{l}_i) = \frac{G_F M_Z^3}{6\sqrt{2}\,\pi}(a_i^2 + b_i^2) \tag{20}$$

for leptons and

$$\Gamma_0 = \Gamma(Z^0 \to q_i\bar{q}_i) = \frac{G_F M_Z^3}{2\sqrt{2}\,\pi}(a_i^2 + b_i^2) \tag{21}$$

for quarks, the difference being a factor of 3 due to color.

As in previous sections we will normalize the three-body decay widths to Γ_0. Once this is done, all the dependence on the boson-fermion coupling drops out[14] and we can relate the two ratios $(\Gamma/\Gamma_0)(W)$ and $(\Gamma/\Gamma_0)(Z^0)$ in a simple fashion. Furthermore, since the two Z^0 decays (iii) and (iv) involve only the Abelian amplitude as defined earlier (see Fig. 1), we can relate them either to $W \to q\bar{q}\gamma$ with $Q=0$ or, equivalently, to $W \to q\bar{q}g$.

We start with $Z^0 \to q_i\bar{q}_i g$. In terms of $\Gamma(W \to q\bar{q}g)$, $\Gamma_0(W \to q\bar{q})$, and $\Gamma^0(Z^0 \to q\bar{q})$ which are given in Eqs. (18), (8), and (21), respectively, we can write

$$\frac{1}{\Gamma_{Z^0}}\Gamma(Z^0 \to q\bar{q}g) = \frac{1}{\Gamma_W}\Gamma(W \to q\bar{q}g) \tag{22}$$

[where $\Gamma_{Z^0} = \Gamma(Z^0 \to q\bar{q})$, $\Gamma_W = \Gamma(W \to q\bar{q})$] an equality which holds for the single- and double-differential decay rates also.

For the decays involving a photon we have

$$\frac{1}{\Gamma_{Z^0}}\Gamma(Z^0 \to q_i\bar{q}_i\gamma) = \frac{1}{\Gamma_W}\Gamma(W \to q_i\bar{q}_j\gamma)\Big|_{Q=0}. \tag{23}$$

Also

$$\frac{1}{\Gamma_{Z^0}}\Gamma(Z^0 \to l^+l^-\gamma) = \frac{1}{Q_i^2\Gamma_{Z^0}}\Gamma(Z^0 \to q_i\bar{q}_i\gamma) = \frac{3}{4}\frac{\alpha}{\alpha_s\Gamma_{Z^0}}\Gamma(Z^0 \to q\bar{q}g). \tag{24}$$

The factors $\frac{3}{4}$, $\frac{1}{3}$, and $\frac{1}{12}$ quoted in the figure captions are obtained from Eqs. (22) and (24).

As an example of a purely leptonic process which illustrates the difference between the Abelian and non-Abelian amplitudes, in Fig. 8 we plot $(1/\Gamma_0)\,d\Gamma/dy$, essentially the energy distribution of the electrons, for the two decays $W^- \to e^-\bar{\nu}_e\gamma$ and $Z^0 \to e^-e^+\gamma$. Clearly, the electron in W decay has a rather flat energy distribution, while in Z^0 decay it is peaked towards larger energies, i.e., small y. This behavior is explained by noticing that in the doubly differential decay rate the only difference between $W \to e\bar{\nu}_e\gamma$ and $Z^0 \to e^-e^+\gamma$ is the factor $y^2/(x+y)^2$ which smooths out the y distribution and, in addition, suppresses $W \to e\bar{\nu}_e\gamma$, as seen in Fig. 8, relative to $Z^0 \to e^-e^+\gamma$.

V. CONCLUSIONS

In our study of the decay processes (i) to (iv), clearly the first one is the most interesting and exhibits the strange behavior of vanishing along a line in the Dalitz plot (Fig. 3). By crossing we can make a connection with the production amplitude

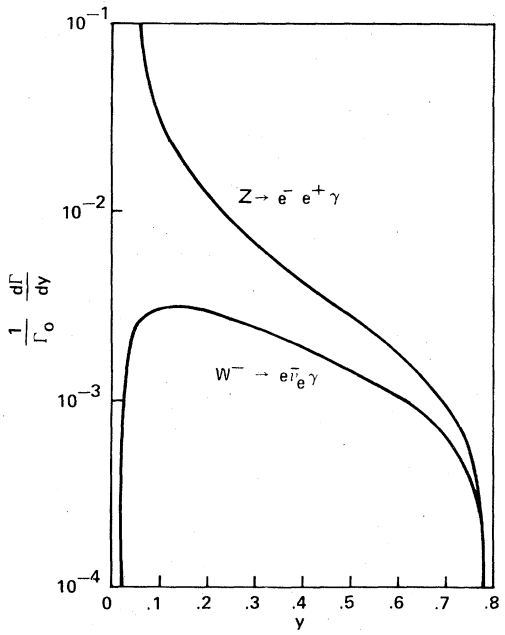

FIG. 8. The differential decay rates $d\Gamma/dy$ for $Z^0 \to e^-e^+\gamma$ and $W^- \to e\bar{\nu}_e\gamma$ normalized to $\Gamma(Z^0 \to e^-e^+)$ and $\Gamma(W^- \to e\bar{\nu}_e)$, respectively, with the cutoff $\epsilon = 0.1$. These curves are obtained from Eq. (12) with $Q=0$, $Q_i=-1$ for Z^0 decay, and $Q = Q_i = -1$ for W^- decay.

for $q_i\bar{q}_j \to W^-\gamma$ where it was found[8] that $(d\sigma/d\cos\theta)$ $(q_i\bar{q}_j \to W^-\gamma)$ vanishes at $\cos\theta = -(1-2Q_i/Q)$. Again, the position of this "zero angle" and the slope of the "zero line" in $W^- \to q_i\bar{q}_j\gamma$ [see Eq. (11)] depend on the ratio of quark to W charges, Q_i/Q. As we discussed in Sec. II, the vanishing of the amplitudes can be traced to the factorization property of the full amplitude which is the sum of the three Feynman diagrams in Fig. 2. Factorization seems to require a triboson coupling as given by non-Abelian gauge theories (Yang-Mills coupling with $\kappa = 1$). Such a factorization was obtained[6] earlier in the photoproduction of W bosons off quarks, but the implications were not explored. More recently, the factorization of certain scattering amplitudes in non-Abelian gauge theories, and the presence of zeros in the angular distributions were discussed[15] in a more general approach with different groups—for example, there is a factorization (but no zero) in $q\bar{q} \to gg$, where again the trigluon coupling is responsible for the factorization.

In the case of processes (i) and (iii), it should be noted that we are not doing radiative corrections to the two-body decays, which would, of course, require virtual photon corrections along with soft-photon emission. These corrections have been done[16]; we require the detection of the photon to identify the three-body-decay process. We chose x and y as our independent variables, but, of course, the photon energy is given by

$$x+y=\frac{2E_\gamma}{M_W}. \tag{25}$$

and similarly for the gluon. The zero occurs not at a unique value of E_γ but for a whole range given by

$$E_\gamma=\frac{Q}{Q_i}(M_W/2-E_{\bar{q}})=\frac{Q}{Q_j}(M_W/2-E_q). \tag{26}$$

Experimentally, the detection of such a zero requires distinguishing a quark jet from an antiquark jet for the purpose of identifying x and y (one may, of course, turn this argument around). If no distinction is made, then we need to fold the x and y distributions. In that case, it is easy to see that no zeros are present unless $Q_i = Q_j$.

We discussed the rest of the processes (ii)–(iv) briefly because we could obtain them with little effort from (i). Our purpose was to compare and contrast processes with and without the triboson coupling. We conclude that (ii)–(iv) have smooth x and y distributions, as can be seen from Figs. 4–6. While process (i) can be used to measure the magnetic moment of the $W^\pm$ through its parameter κ, as we are advocating here, measuring (ii) and (iv) would confirm our present ideas about three-jet events in e^+e^- collisions and extend them to the weak interactions and, of course, to higher energies.

The advantage of looking at $W^\pm$ decays over associated production[8] or photoproduction[6] is that one may study the decays of the W bosons independently of how they are produced. In particular, LEP may be a good source, via $e^+e^- \to W^+W^-$, while pp and $\bar{p}p$ machines may be too "messy" to allow detailed study of rare decay modes such as $W \to q\bar{q}\gamma$ with a branching ratio of 0.1 to 0.01 percent depending on ϵ (see Fig. 7). Clearly, a very rich source of weak bosons is needed for such studies.

Z^0 factories are expected to be an even richer source of weak neutral bosons and it may be disappointing that the decays (iii) and (iv) are not as exciting because no triboson coupling is involved. One can, nevertheless, do interesting three-jet physics beyond the confirmation of our present ideas and the extension mentioned above for $Z^0 \to q\bar{q}g$. If one can distinguish gluon jets, then Z^0 factories have the advantage of studying the decay

$$Z^0 \to ggg, \tag{27}$$

which proceeds through the Feynman diagrams shown in Fig. 9 (the two-gluon mode $Z^0 \to gg$ vanishes). The branching ratio is of order $\alpha_s^3 \sim 0.6\%$, not too small for a Z^0 factory. Calculations are in progress for the ggg, $\gamma\gamma\gamma$, and $gg\gamma$ decay modes of the Z^0, and will be reported elsewhere.[17]

ACKNOWLEDGMENTS

We wish to thank F. Halzen and M. A. Samuel for discussions related to this work. This research was supported by the U. S. Department of Energy Contract No. EY-76-S-05-5074.

APPENDIX A: SPIN-0 QUARKS

To see if the factorization of the $W \to q\bar{q}\gamma$ amplitude still holds if the quarks had spin = 0, we calculate this decay amplitude using scalar electroweak interactions. The vertices are

$$A_\mu\phi_i(q_1)\phi_i^\dagger(q_2): \; -ieQ_i(q_1+q_2)_\mu, \tag{A1}$$

$$W_\mu\phi_i(q_1)\phi_j^\dagger(q_2): \; -iG(q_1+q_2)_\mu, \tag{A2}$$

$$W_\mu A_\nu\phi_i\phi_j^\dagger: \; ieG(Q_i-Q_j)g_{\mu\nu}. \tag{A3}$$

There are now four Feynman diagrams—the three shown in Fig. 2, plus a contact or seagull term given by (A3). The amplitude is

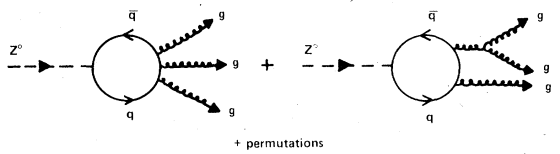

FIG. 9. Feynman diagrams for the decay $Z^0 \to ggg$.

$$\mathfrak{M}(\text{spin}=0\ \text{quarks}) = -ieG\epsilon_\gamma^\mu\epsilon_W^\nu\left\{\frac{Q_i}{l_1^2}(2q_1+k)_\mu(p-2q_2)_\nu+\frac{Q_j}{l_2^2}(2q_2+k)_\mu(2q_1-p)_\nu\right.$$
$$+\frac{Q}{h^2-M_W^2}[2p_\mu(q_1-q_2)_\nu-(p+k)\cdot(q_1-q_2)g_{\mu\nu}-2(q_1-q_2)_\mu(q_1+q_2)_\nu]$$
$$\left.-(Q_i-Q_j)g_{\mu\nu}\right\}, \tag{A4}$$

which is, of course, gauge invariant since $Q=Q_i+Q_j$.

After some algebra, we find

$$\mathfrak{M}(\text{spin}=0\ \text{quarks}) = 4ieG\left(Q_i-Q\frac{k\cdot q_1}{k\cdot p}\right)(q_{1\mu}q_{2\nu}/l_1^2+q_{2\mu}q_{1\nu}/l_2^2+g_{\mu\nu}/2)\epsilon_\gamma^\mu\epsilon_W^\nu. \tag{A5}$$

Comparing (A5) with Eq. (3), we see that the *same* factor $Q_i-Q(k\cdot q_1)/(k\cdot p)$ can be pulled out of the full amplitude, which implies that the zero will occur at the same place irrespective of the spin of the quarks.

APPENDIX B: ARBITRARY κ

Implicit in all our calculations so far is the assumption that the W-γ-W coupling is given by gauge theories. This vertex enters in the last Feynman diagram of Fig. 2, and the results are substantially altered if we use a different coupling, which we do following the standard technique of using a magnetic-moment parameter κ (see Ref. 7), in terms of which the magnetic moment μ_W of the W boson is given by

$$\mu_W=\frac{e}{2M_W}(1+\kappa). \tag{B1}$$

In gauge theories $\kappa=1$ (or, since $g=1+\kappa$, $g=2$). For arbitrary κ, we must add terms proportional to $(1-\kappa)$ in the W-γ-W vertex, which changes the contribution of the last diagram in Fig. 2.

To use the decay $W\to q\bar{q}\gamma$ or $W\to e\bar{\nu}\gamma$ as a means of measuring μ_W, it is helpful to know the doubly differential decay rate $d^2\Gamma/dx\,dy$ for arbitrary κ. We find

$$\frac{1}{\Gamma_0}\frac{d^2\Gamma}{dx\,dy}=\frac{\alpha}{2\pi}\left\{\left[Q_i-Q\frac{x}{x+y}\right]^2\frac{(x-1)^2+(y-1)^2}{xy}\right.$$
$$+(1-\kappa)Q\left[Q_i-Q\frac{x}{x+y}\right]\left[\frac{y-x}{y+x}\right]$$
$$\left.+\frac{(1-\kappa)^2Q^2}{8(x+y)^2}[4xy+(x^2+y^2)(1-x-y)]\right\}, \tag{B2}$$

which should be compared with Eq. (9). It is clear that the additional terms spoil the zero which is present when $\kappa=1$, its gauge-theory value.

*Present address: Physics Department, University of Texas, Austin, Texas.

†Present address: Lawrence Livermore Laboratory, Livermore, California.

[1]For a recent historical survey, see P. Q. Hung and C. Quigg, Report No. Fermilab-Pub-80-24-THY, 1980 (unpublished).

[2]R. F. Peierls, L. T. Trueman, and L. L. Wang, Phys. Rev. D 16, 1397 (1977); F. Paige, in *Proceedings of Topical Workshop on the Production of New Particles in Super High Energy Collisions, Madison, Wisconsin, 1979,* edited by V. Barger and F. Halzen (University of Wisconsin, Madison, 1979).

[3]R. W. Brown and K. O. Mikaelian, Phys. Rev. D 19, 922 (1979); R. W. Brown, D. Sahdev, and K. O. Mikaelian, *ibid.* 20, 1164 (1979).

[4]J. Ellis, M. K. Gaillard, and G. G. Ross, Nucl. Phys. B111, 253 (1976); K. Koller, H. Krasemann, and T. F. Walsh, Z. Phys. C 1, 71 (1979).

[5]Quark masses do not spoil the factorization: the algebra is more tedious, but the results are remarkably similar; we find

$$\mathfrak{M}=\frac{-ieg}{2\sqrt{2}}\left(Q_i-Q\frac{k\cdot q_1}{k\cdot p}\right)\epsilon_\gamma^\mu\epsilon_W^\nu\,\bar{u}(q_1)$$
$$\left[\gamma_\mu\frac{1}{\not{l}_1-m_1}\gamma_\nu(1-\gamma_5)-(1+\gamma_5)\gamma_\nu\frac{1}{\not{l}_2+m_2}\gamma_\mu\right]v(q_2).$$

[6]K. O. Mikaelian, Phys. Rev. D 17, 750 (1978).

[7]T. D. Lee and C. N. Yang, Phys. Rev. 128, 885 (1962).

[8]K. O. Mikaelian, M. A. Samuel, and D. Sahdev, Phys. Rev. Lett. 43, 746 (1979).

[9]We have suppressed Cabibbo angles in Eq. (6). For $W^-\to d\bar{u}\gamma$ and $W^-\to s\bar{u}\gamma$, Eq. (6) must be multiplied by $\cos^2\theta_C$ and $\sin^2\theta_C$, respectively.

[10]By introducing only one parameter ϵ, we treat all cuts symmetrically—see Fig. 3 and J. Ellis *et al.* in Ref. 4. Collinear events are also eliminated.

[11]T. G. Rizzo, Brookhaven Report No. BNL-26286, 1979 (unpublished).

[12]P. Hoyer *et al.*, Nucl. Phys. B161, 349 (1979); H. P. Nilles, Phys. Rev. Lett. 45, 319 (1980).

[13]D. P. Barber *et al.*, Phys. Lett. 89B, 139 (1979); R. Brandelik *et al.*, Report No. DESY 80/40, 1980

(unpublished).
[14]This is true as long as we neglect quark masses and consider only spin-averaged quantities.
[15]Z. Dongpei, Phys. Rev. D 22, 2266 (1980).
[16]D. Albert *et al.*, Nucl. Phys. B166, 460 (1980); E. Ma, talk given at the XXth International Conference in High Energy Physics, Madison, Wisconsin, 1980 (unpublished).
[17]M. L. Laursen, K. O. Mikaelian, and M. A. Samuel, work in preparation.